Science in China Series E: Technological Sciences

www.scichina.com
tech.scichina.com
www.springerlink.com

Seismic cyclic loading test of SRC columns confined with 5-spirals

WENG ChengChiang[1†], YIN YenLiang[2], WANG JuiChen[2] & LIANG ChingYu[1]

[1] Department of Civil Engineering, Chiao Tung University, Hsinchu 30050, China;
[2] Ruentex Group, Taibei 10492, China

Presented herein is an experimental study on seismic resistance of rectangular steel reinforced concrete (SRC) columns confined with a new type of multi-spiral cage. The multi-spiral cage is a device of five interconnected spirals, named "5-spirals", with a large spiral at the center and four small ones at the corners. The innovation of applying the 5-spirals to SRC column is to take its superiority in concrete confinement and efficiency in automatic production for the precast construction industry. Four full-scale SRC columns were tested under horizontal cyclic loading. All of the tested columns were capable of sustaining a drift angle up to 6% radians. The hysteresis loops observed from the cyclic loading tests indicated that the spirally confined SRC columns demonstrated excellent performances in both strength and ductility. The test results suggested that with significant saving of the confinement steel, the newly innovated 5-spirals can be successfully applied to the precast rectangular SRC columns.

steel reinforced concrete, rectangular SRC column, precast construction, 5-spirals, concrete confinement, cyclic loading test, seismic resistance

1 Introduction

The design of steel reinforced concrete (SRC) structures is aimed at effectively combining the structures of steel (S) and reinforced concrete (RC) so that it may have advantages of the two structures. A meticulously designed SRC structure may not only enjoy advantages of S and RC, but also apply the two structures in a supplementary way to reach the safer and more cost-effective goals. In a eugenic perspective, a properly designed SRC structure is like a "eugenic baby" as an outcome of the "marriage" of the S structure and the RC structure[1].

For the SRC column, concrete cladding the steel surface performs the following functions: (1) provision of fireproof coating of the steel column; (2) enhancement of rust protection of the steel column; (3) reduction in probability of buckling of the steel column. Compared with the pure

Received December 13, 2006; accepted June 19, 2007
doi: 10.1007/s11431-008-0067-z
†Corresponding author (email: frankweng@mail.nctu.edu.tw)

steel column, the SRC column uses the compression resistance advantage of concrete to improve the compressive strength of the column, which helps cut cost, reduce the application of ultra-thick steel plate and minimize the probability of welding defects. The SRC column has larger cross-section moment of inertia than the pure steel column and effectively reduces lateral displacement of the building. Against the hike in steel prices, the substitution of the SRC column for the pure steel column will contribute to cost reduction. Compared with the conventional RC column, the application of the SRC column reduces the cross-sectional area of the column and increases the floorage of the building. Furthermore, as the steel section in the SRC column has the function of confining concrete, it may reduce the hoop demand of the SRC column to be more cost-effective[1].

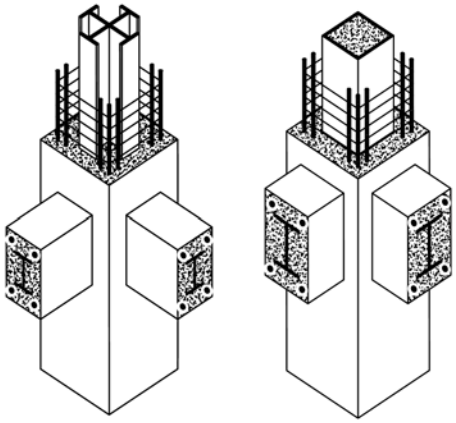

Figure 1 Rectangular SRC columns tied with rectangular hoops[1]

As shown in Figure 1, the lateral reforcements for the rectangular SRC columns in the engineering field are largely the rectangular hoops. As it takes much time and work to bond the rectangular hoops, the use of spirals will substantially reduce the time and manpower required for the bonding of the hoops. Spirals are continuous, unlike the rectangular hoops which are separate and need hooks for fixing at the corner. So the spirals enjoy better confining effect upon concrete than the rectangular hoops do and save a considerable amount of steel as they do not need hooks. However, although the confining effect and economic benefit of the spirals are both superior to the rectangular hoops, the spirals fail to provide effective confinement to concrete at the four corners of the rectangular columns. That is why the spirals are seldom used for the rectangular column in the engineering field.

As shown in Figure 2, the 5-spiral configuration for confining hoops will effectively solve the problem of unconfined concrete at the corners of rectangular SRC columns. The innovative concept of applying the 5-spirals in rectangular columns was put forward by Dr. Y. L. Yin, CEO of Ruentex Group, thus also called "Yin's spirals." The 5-spiral cage is a device of five interconnected spirals, with a large spiral at the center and four small ones at the corners. The innovative configuration breaks through the application restriction of the conventional spirals to circular cross-sectional columns, overcomes the shortcomings of spiral application to rectangular cross-sectional columns and facilitates sound confinement of spirals to concrete at the corners of the rectangular column. Moreover, as the 5-spirals are manufactured with automatic machines in the factory, they are expected to substantially reduce manpower in bonding of conventional hoops and shorten the construction period. Being most cost-effective, the 5-spirals are suitable for precast construction.

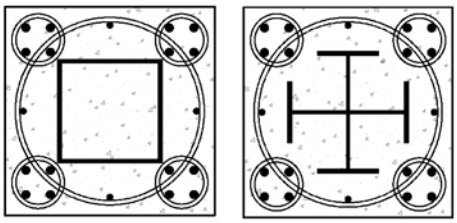

Figure 2 Rectangular SRC columns confined with the newly innovated 5-spirals.

For the 5-spirals as confining hoops of rectangular reinforced concrete (RC) columns, Chang et al.[2, 3] conducted a series of axial compression tests, which demonstrated that the 5-spirals can be successfully applied to rectangular RC columns. The test results suggested that the 5-spirals

have good confining effect on core concrete of the RC columns, with tangibly better toughness than the columns tied with the conventional rectangular hoops. Therefore, this study will further explore the possibility of applying the newly innovated 5-spirals to rectangular SRC columns.

With the presence of steel section in the SRC columns, the way concrete is confined on the cross section is different from general RC columns. Figures 3(a) and (b) demonstrate the confinement of steel section to the concrete in the SRC columns. As shown in the figures, Weng and Yen[4] considered the confinement effect of the steel flange on concrete in the SRC column, and categorized the concrete of the SRC column into three areas: (1) the highly confined area, the dark grey part in Figures 3(a) and (b), concrete confined between the steel flange and the web plate; (2) the ordinary confined area, the light grey part in Figures 3(a) and (b), concrete in the hoop, but not including the foregoing area surrounded by the steel flange and the web plate; (3) the unconfined area, the blank part in Figures 3(a) and (b), concrete peripheral to the hoop. Effects on concrete compressive strength vary with extent of confinement of concrete in all areas in the SRC column.

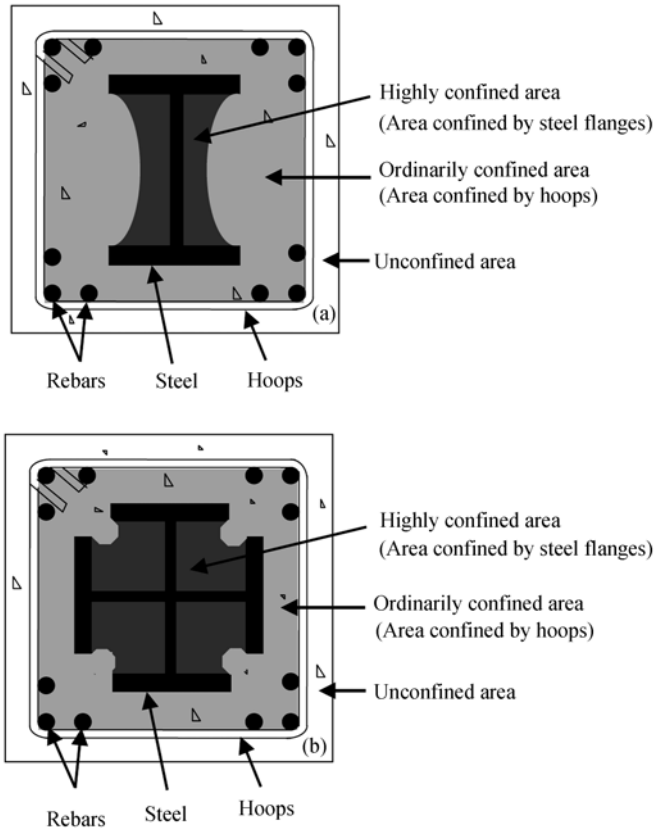

Figure 3 Conditions of concrete confinement in SRC columns: highly confined area versus ordinarily confined area[4]. (a) SRC column with H-type steel; (b) SRC column with cross-H type steel.

On SRC column-related researches, Japanese scholars Nakamura and Wakabayashi[5] held in 1976 that S and RC were two separate members in designing an SRC structure, and they could be simply added after calculations of individual strength. In the same year, a US scholar Furlong[6] proposed conversing reinforced concrete to equivalent steel with conversion factors and using the design formulas of AISC (American Institute of Steel Construction) Specification. Comparing

calculation methods for compressive strength of SRC members of the ACI (American Concrete Institute) Code and the AISC Specification, Furlong[7] found in 1983 that the calculation results of ACI were conservative and the calculation process was rather complicated. Hamdan et al.[8] discussed effects of concrete strength, confinement effect and steel surface conditions on the steel of the SRC column and RC interface strength in 1991. Wakabayashi[9] studied application of high tension steel to SRC columns in 1992. Mirza and Skrabek[10, 11] made respective studies into mechanical behaviors of SRC short and slender columns subjected to axial force and bending moment in 1991 and 1992. Ricles and Paboojian[12] simulated SRC column behaviors under seismic force with experiments in 1994. Their findings suggested that the strength and toughness of SRC columns were affected by the confinement status of core concrete, and the ability of hoops to effectively confine the core concrete might avoid premature buckling of main reinforcement. Mirza and Hyttinen[13] conducted tests on 16 groups of SRC columns under combined actions of axial force and bending moment in 1994, and applied the finite element method to compare the test results. Mirza and Tikka[14] discussed changes in flexure stiffness of the SRC column subjected to bending of the strong and weak axes and deducted the flexural stiffness value of the rectangular slender SRC column in 1999. Mirza and Lacroix[15] made a series of comparative analyses for the strength of concrete-encased SRC columns in 2004. Tikka and Mirza[16,17] went further in 2005 and 2006 by using parameter variations to deduct the nonlinear flexural stiffness of the slender SRC column subjected to the strong axis bending.

The research team had previously completed a series of axial compression tests[18] on full-scale 5-spiral rectangular SRC short columns and found that the 5-spirals had sound concrete confinement, could improve the strength and toughness of SRC columns and effectively overcome the shortcoming of complicated construction for the conventional rectangular hoops. In an attempt to discuss mechanical behavior and seismic resistance of the 5-spiral rectangular SRC column under cyclic actions of seismic force, the research team conducted cyclic loading tests on four full-scale SRC columns, discussed their strength and toughness under horizontal seismic force, used them as the basis for evaluation of the seismic resistance of the SRC columns confined with the newly innovated 5-spirals, and provided appropriate guidelines for future engineering applications.

2 Design provisions of seismic confining hoops for SRC columns

This section gives a brief account of provisions of design of seismic confining hoops for SRC columns in the ACI-318 Code[19], the AISC-Seismic Provisions[20] and the newly released Taiwan Design Code for SRC Structures (hereinafter referred to as the Taiwan SRC Code)[21]. What merits attention is the three foregoing codes which did not take into account changes in the steel flange width in the SRC column section when calculating confining hoop consumption of concrete in the SRC column, so the rationality of their design formulas awaits further discussion[22].

2.1 ACI-318 Code

The ACI-318 Code (2005) is in extensive application for structural design of SRC columns, but it has no explicit provision of confining hoops of the SRC column. The seismic provision in Chapter 21 of the Code stipulates in the use of general RC columns confined with spirals, its specific volume ratio of spiral ρ_s shall not be less than the provisions of the formulas below:

$$\rho_s = 0.45\left(\frac{A_g}{A_c} - 1\right)\left(\frac{f_c'}{f_{yh}}\right) \tag{1}$$

and

$$\rho_s = 0.12\left(\frac{f_c'}{f_{yh}}\right), \tag{2}$$

where f_c' is the compressive strength of concrete (for ϕ150×300 mm standard cylinder test piece), f_{yh} is the yield strength of the confining hoop, A_g is the gross area of the SRC column, and A_c is the core area confined with hoops.

Moreover, the seismic provision of Chapter 21 of the ACI-318 Code stipulates in the use of the RC column confined with rectangular hoops, their minimum confining hoops A_{sh} shall not be less than the provisions of the following two formulas:

$$A_{sh} = 0.3sh_c\left(\frac{f_c'}{f_{yh}}\right)\left(\frac{A_g}{A_{ch}} - 1\right) \tag{3}$$

and

$$A_{sh} = 0.09\, sh_c\left(\frac{f_c'}{f_{yh}}\right), \tag{4}$$

where s is the spacing of the confining hoops, h_c is the width of core area confined with hoops, and A_{ch} is the core area confined with hoops.

2.2 AISC-Seismic Provisions

The requirements for hoops of concrete-encased SRC column in the AISC-Seismic Provisions (2005) stipulate in the use of the SRC column confined with rectangular hoops, its minimum confining hoops A_{sh} shall be calculated in the following formula:

$$A_{sh} = 0.09\, sh_c\left(\frac{f_c'}{f_{yh}}\right)\left(1 - \frac{f_{ys}A_s}{P_n}\right), \tag{5}$$

where f_{ys} is the yield strength of the steel, A_s is the steel area, and P_n is the nominal axial compression strength of the SRC column. What merits attention is formula (5) which follows the basic framework of formula (4), but as steel in the SRC column area can provide part of the axial compressive strength, $(1-f_{ys}A_s/P_n)$ in formula (5) is a reduction coefficient on the ground that the steel section bears part of the SRC column axial force, indirectly reducing the compression status of the concrete as basis for reducing SRC column hoop consumption.

2.3 Taiwan SRC Code

As Taiwan building code did not stipulate design of SRC structures before 2004, architects and engineers lacked a set of standards in design of SRC structures. Based on the need, the Architecture & Building Research Institute (ABRI) of Taiwan entrusted the Structural Engineering Society with research of SRC design code, and Professor C.C. Weng with the Department of Civil Engineering of Chiao Tung University acted as project leader.

After years' efforts of the research team and extensive solicitation of scholars and experts, the draft SRC design code was passed by the Taiwan Construction and Planning Agency (CPA) at the

end of 2003. The CPA released some revised articles of the Building Technology Act on January 16th, 2004, which added a "Chapter Seven: Steel Reinforced Concrete Structures" to the building structure part and made explicit provisions of SRC structural design from Articles 496 to 520. Then, the CPA announced that the "Design Code and Commentary for Steel Reinforced Concrete Structures"[21] (or "Taiwan SRC Code") become officially effective from July 1st, 2004. Henceforth, Taiwan SRC structure designers have explicit SRC structure design code to comply with[23].

With reference to similar practice of AISC-Seismic Provisions, Taiwan SRC Code stipulates that the confining hoop consumption A_{sh} of SRC columns confined with rectangular hoops shall not be less than what is required in the following two formulas:

$$A_{sh} = 0.3sh_c\left(\frac{f_c'}{f_{yh}}\right)\left(\frac{A_g}{A_{ch}}-1\right)\left[1-\left(\frac{A_s f_{ys}}{(P_n)_u}\right)\right] \tag{6}$$

and

$$A_{sh} = 0.09\,sh_c\left(\frac{f_c'}{f_{yh}}\right)\left[1-\left(\frac{A_s f_{ys}}{(P_n)_u}\right)\right]. \tag{7}$$

In the foregoing formula, $(P_n)_u$ is the nominal axial capacity of the SRC column, whose calculation is done in line with the following formula:

$$(P_n)_u = f_{ys}A_s + 0.85\,f_c'\,A_c + f_{yr}A_r, \tag{8}$$

where f_{yr} and A_r are the yield strength and the total cross-sectional area of the longitudinal reinforcement, respectively.

Further, in arranging spirals, Taiwan SRC Code proposes that the volume ratio of SRC column spiral, ρ_s, shall not be less than the requirement given in the following two formulas:

$$\rho_s = 0.45\left(\frac{A_g}{A_c}-1\right)\left(\frac{f_c'}{f_{yh}}\right)\left[1-\left(\frac{A_s f_{ys}}{(P_n)_u}\right)\right] \tag{9}$$

and

$$\rho_s = 0.12\left(\frac{f_c'}{f_{yh}}\right)\left[1-\left(\frac{A_s f_{ys}}{(P_n)_u}\right)\right], \tag{10}$$

where $(P_n)_u$ is the nominal axial capacity of the SRC column, whose calculations are done in line with formula (8).

3 Cyclic loading tests of 5-spiral rectangular SRC columns

3.1 Specimen planning

The tests were aimed at investigating the mechanical behavior and seismic resistance of the 5-spiral rectangular SRC columns. Seismic resistance of SRC columns was tested on four full-scale specimens subjected to cyclic loading, with the cross-sectional area of SRC columns being 600 mm×600 mm and height being 3250 mm. The specimen designation, hoop spacing, consumption and design method are shown in Table 1, and the cross sections of the specimens are shown in Figure 4. The details of the front and top views and the arrangement of the reinforcing bars of the specimens are shown in Figures 5 and 6, respectively.

Table 1 Design details of SRC columns tested in this study

SRC column cross-section	Specimen designation	Size of spiral		Spacing of spiral (mm)	Volume ratio of spiral ρ_s	Unit weight of spiral (N/m)	Spiral reduction factor	Design basis
		small	big					
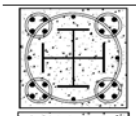	C-SRC1-TWN-95	#3	#4	95	0.99%	283	0.79	Taiwan SRC Code
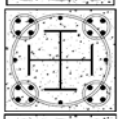	C-SRC2-WENG-115	#3	#4	115	0.81%	235	0.65	Weng's Formula
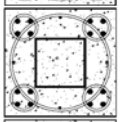	C-SRC3-TWN-95	#3	#4	95	0.99%	283	0.79	Taiwan SRC Code
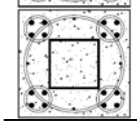	C-SRC4-WENG-110	#3	#4	110	0.85%	245	0.68	Weng's Formula

Note: (1) SRC column dimensions: Height: 3550 mm; cross-section: 600 mm × 600 mm; RC foundation size: 2500 mm× 1800 mm× 750 mm; full height of the specimen including RC foundation: 4300 mm; top portion of SRC column is enlarged to 600 mm× 600 mm× 900 mm to connect the MTS actuator. (2) Steel section in SRC column: A572 Gr.50; cross H: 2H350 × 175 × 6 × 9; ρ = 2.91%; box section: □275 × 275 × 10 × 10; ρ = 2.94%. (3) Longitudinal bar in SRC column: 16 #8 (D25); ρ_r = 2.25%; SD420; supplementary longitudinal bar: 4 #4 (D13) as required by the Taiwan SRC Code. (4) Spiral: #3 (D10), #4 (D13); SD420. (5) Concrete: Normal weight concrete; design compressive strength f_c' = 34.3 MPa.

Before the cyclic loading test, material mechanical tests were conducted on steel, reinforcement and concrete of the specimen. Tensile coupons were cut from the steel plate and tested according to the ASTM standards. Main reinforcement and hoop were taken from the reinforcements as the specimen for tensile strength test. In this experiment, the concrete of the four SRC columns were poured in two batches, concrete specimens of Φ150×300 mm standard cylinders were made for compressive tests. The field measured material strengths of the specimens are shown in Table 2. The preparation of the 5-spirals and the SRC column specimens are shown in Figures 7 and 8. After the assembly of steel section and the reinforcement, strain gauges were affixed to steel section, main reinforcements and hoops near the plastic hinge location at the column base.

In this study, the main design parameters included steel shape, hoop spacing, consumption, column strength and toughness. The cross-H steel section was used for the SRC column specimens C-SRC1 and C-SRC2; welded steel box section was used for the specimens C-SRC3 and C-SRC4. The specimen steel ratio (ratio of steel section area over SRC column section area) was 2.9%, and the steel was A572 Gr.50. The design compressive strength of the normal weight concrete was 34.3 MPa (5000 psi). In each specimen, 16 deformed bars (four at each corner) of # 8(D25) SD420 were used as the longitudinal reinforcements; and the #4(D13) bar was used as the central big spiral, #3(D10) bar was used as the small spirals at the corners. For the design of the confining spirals, Taiwan SRC Code was applied to the specimens C-SRC1 and C-SRC3, while Weng's Formula[22] was applied to specimens C-SRC2 and C-SRC4. The Weng's Formula design method will be discussed in the following section.

3.2 Weng's Formular design method

For the 5-spiral SRC columns, two spiral calculation methods were adopted to arrange the confining spirals of SRC columns: (1) Taiwan SRC Code design method [21]; (2) Weng's Formula

design method[22]. Taiwan SRC Code design method was explained in the foregoing section, the following will give a brief account of Weng's Formula design method.

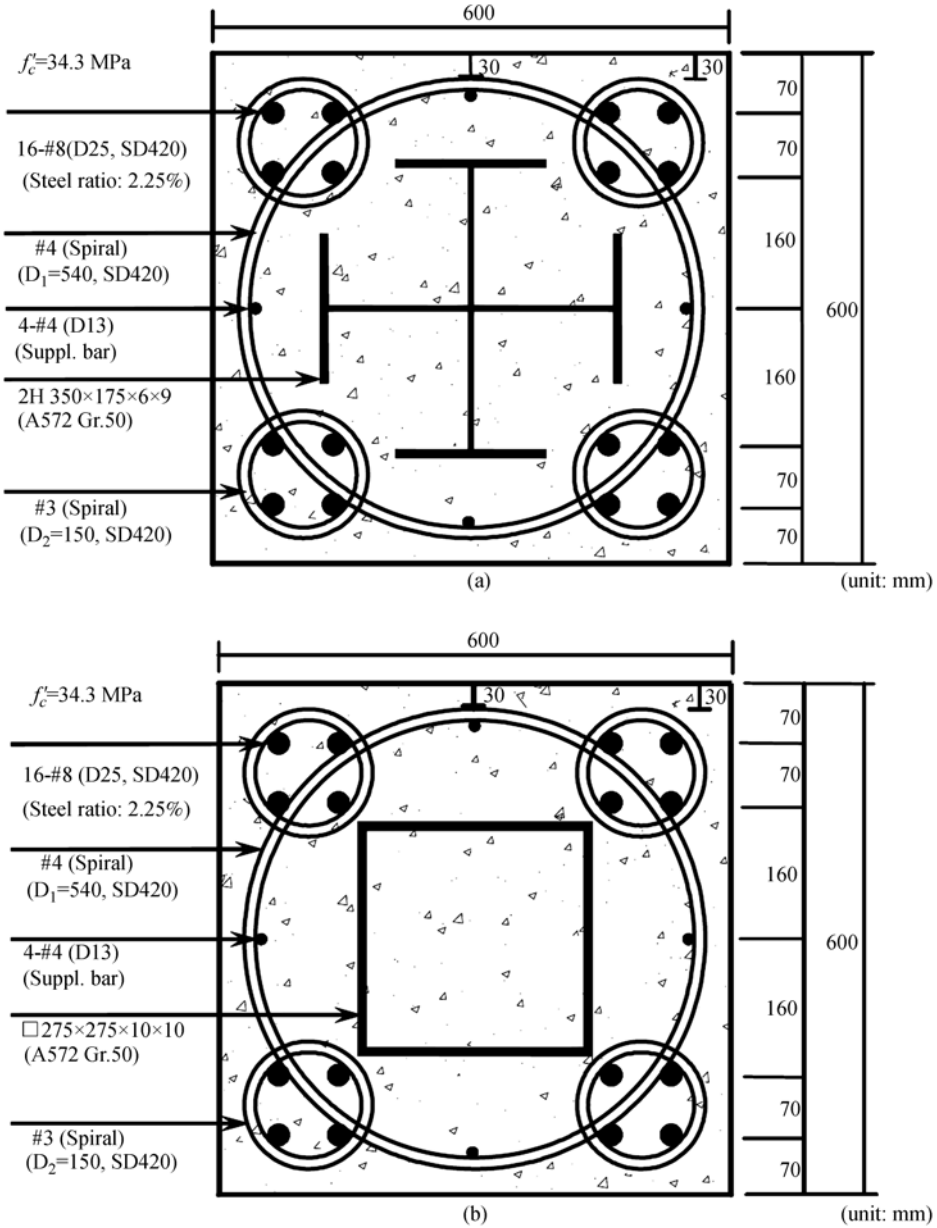

Figure 4 Details of cross-sectional layout of SRC column specimens. (a) SRC column specimens with cross-H steel (C-SRC1, C-SRC2); (b) SRC column specimens with box steel (C-SRC3, C-SRC4).

As shown in Figure 3, compared with the Taiwan SRC Code which stipulates reduced hoops considering steel contribution to bearing axial force of the SRC column, Weng's Formula design method[22] further considers "the contribution of the flanges of steel section in SRC column to concrete confinement," and proposes that "the highly confined concrete" (the dark grey area in Figure 3) in the SRC column can be effectively confined by the flanges of steel section, thus the SRC column hoops can be mainly used to confine "the ordinary confined concrete" (the light

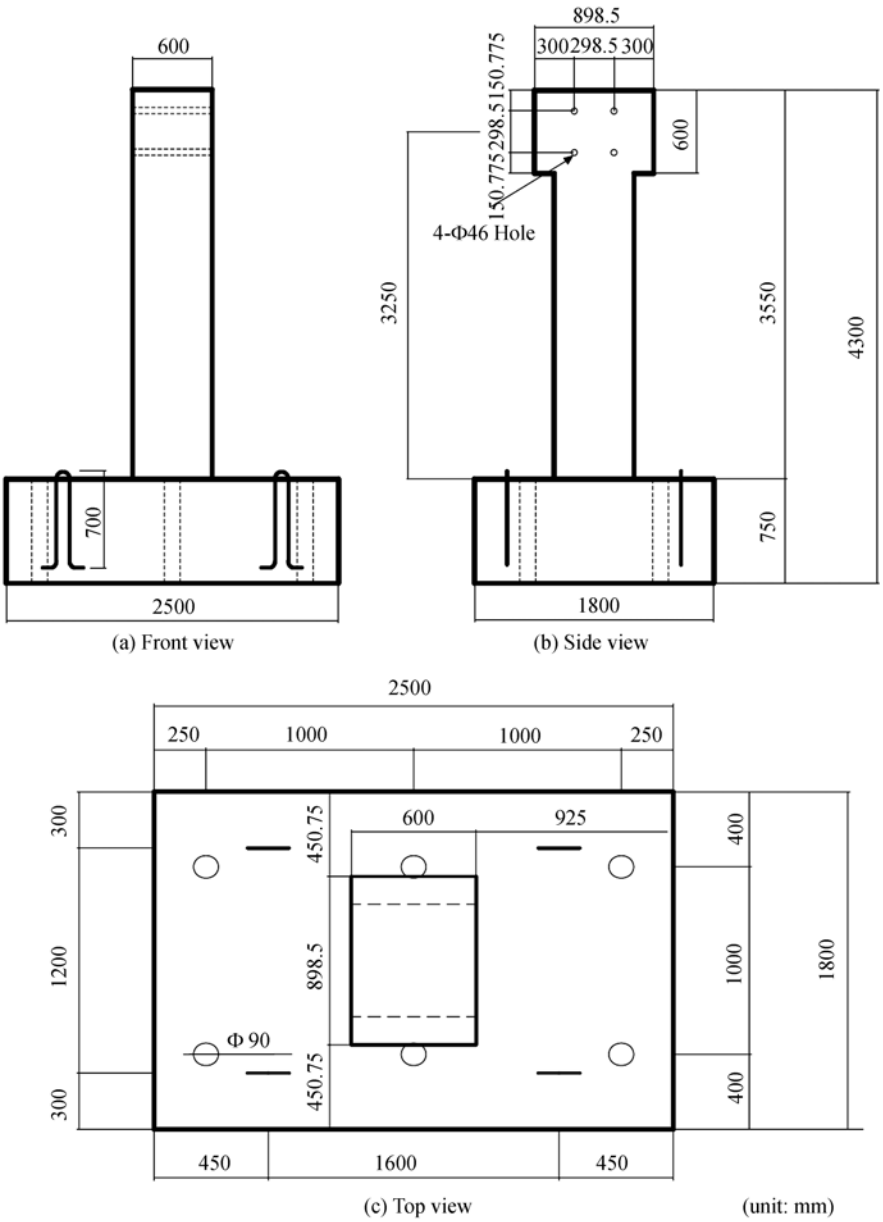

Figure 5 Front and top views of SRC column specimens.

grey area in Figure 3). Therefore, Weng's Formula design method significantly relaxed the consumption of confining hoops of the SRC columns[22]. The following is the design method of the SRC column confining spirals/hoops as proposed by Weng's Formula:

(1) For SRC columns confined with spirals, their hoop volumetric ratio, ρ_s, shall not be less than the provision of the two formulas:

$$\rho_{\mathrm{s}} = 0.45\left(\frac{A_{\mathrm{g}}}{A_{\mathrm{c}}} - 1\right)\left(\frac{f_{\mathrm{c}}'}{f_{\mathrm{yh}}}\right)\left[1 - \left(\frac{P_{\mathrm{s}} + P_{\mathrm{hcc}}}{(P_{\mathrm{n}})_u}\right)\right] \tag{11}$$

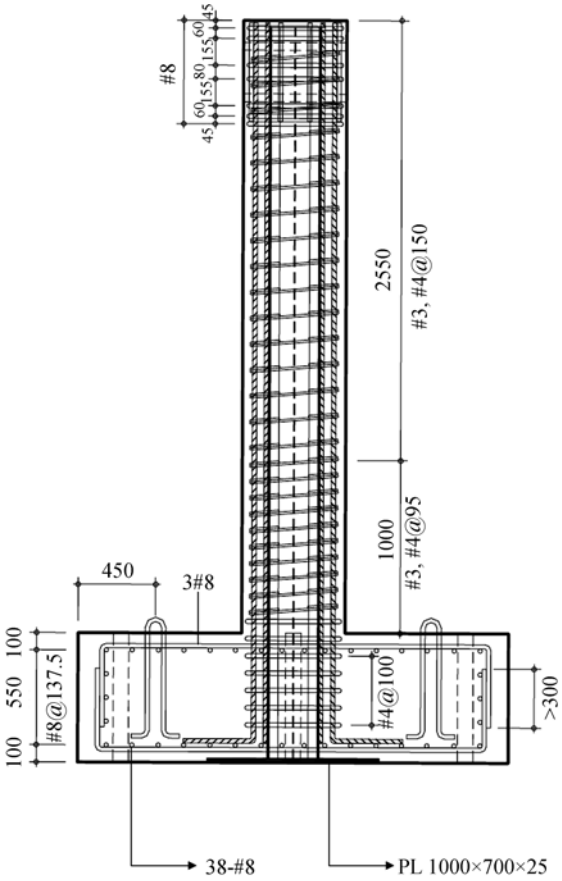

(a) Arrangement of spirals (unit: mm)

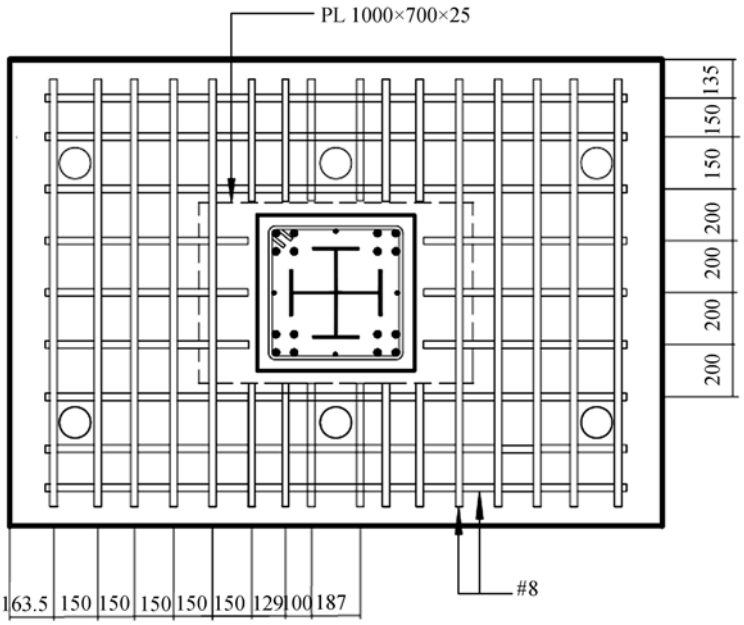

(b) Arrangement of the reinforcing bars (unit: mm)

Figure 6 Arrangement of spirals and reinforcing bars of specimen C-SRC1.

Table 2 The field measured material strengths of the SRC columns

Strength	Material							
	Steel			Reinforcement			Concrete	
	Plate thickness (mm)							
	6	9	10	#3	#4	#8	f_c' (MPa)	
f_y(MPa)	427	457	422	414	444	453	37.3 (C-SRC1, C-SRC2)	40.0 (C-SRC3, C-SRC4)
f_u(MPa)	550	557	538	541	651	649		

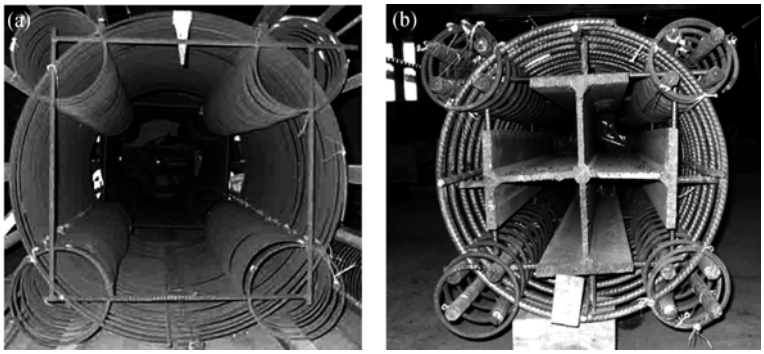

Figure 7 The 5-spirals and the spirally confined SRC column with cross-H steel section. (a) New-type spirals; (b) spirally confined SRC column with cross-H steel section.

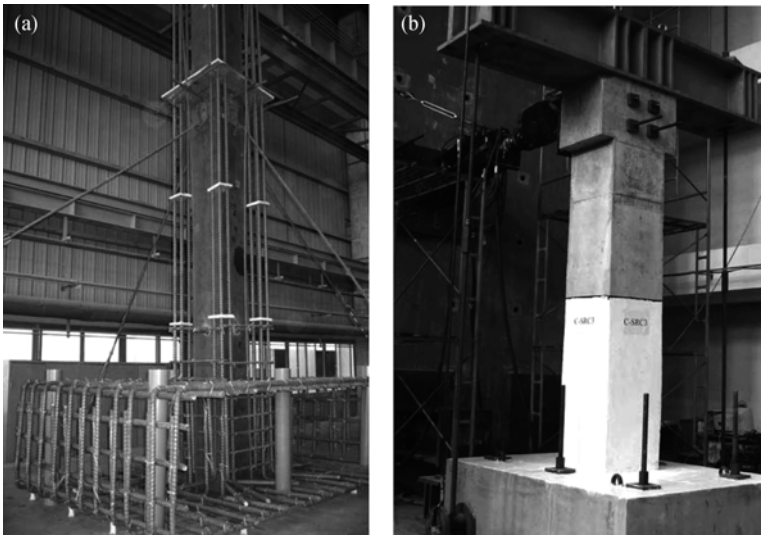

Figure 8 The SRC column in preparation and ready for cyclic test. (a) Grouping steel, main reinforcement and column foundation main reinforcement; (b) grouted SRC column.

and

$$\rho_s = 0.12\left(\frac{f_c'}{f_{yh}}\right)\left[1-\left(\frac{P_s + P_{hcc}}{(P_n)_u}\right)\right]. \tag{12}$$

(2) For SRC columns confined with rectangular hoops, their minimum confining hoops, A_{sh}, shall not be less than the provision of the two formulas:

$$A_{\mathrm{sh}} = 0.3sh_{\mathrm{c}} \left(\frac{f_{\mathrm{c}}'}{f_{\mathrm{yh}}}\right)\left(\frac{A_{\mathrm{g}}}{A_{\mathrm{ch}}} - 1\right)\left[1 - \left(\frac{P_s + P_{\mathrm{hcc}}}{(P_{\mathrm{n}})_u}\right)\right] \tag{13}$$

and

$$A_{\mathrm{sh}} = 0.09\, sh_{\mathrm{c}} \left(\frac{f_{\mathrm{c}}'}{f_{\mathrm{yh}}}\right)\left[1 - \left(\frac{P_{\mathrm{s}} + P_{\mathrm{hcc}}}{(P_{\mathrm{n}})_u}\right)\right]. \tag{14}$$

It is noted that the "medium bracket" in the end of eqs. (11)—(14) stands for the spiral or hoop "reduction factor" in Weng's Formula, where $(P_{\mathrm{n}})_u$ is the nominal axial strength of the SRC column, which is calculated in accordance with formula (8). P_{s} is the steel compressive strength and P_{hcc} is the axial strength of the highly confined concrete, which can be calculated as follows:

$$P_{\mathrm{s}} = f_{\mathrm{ys}} A_{\mathrm{s}}, \tag{15}$$

$$P_{\mathrm{hcc}} = 0.85 f_{\mathrm{c}}' A_{\mathrm{hcc}}, \tag{16}$$

where A_{hcc} is the area of the highly confined concrete of the SRC column as shown in the dark grey part of Figure 3.

3.3 Test devices and test method

The SRC column specimens were assembled in the Ruenhorn precast factory, and then were transported to the structural laboratory of the Department of Civil Engineering of Chiao Tung University for seismic tests. The SRC column loading was conducted in the combination of cyclic lateral force and fixed-value axial compression, with overall test arrangement shown in Figure 9.

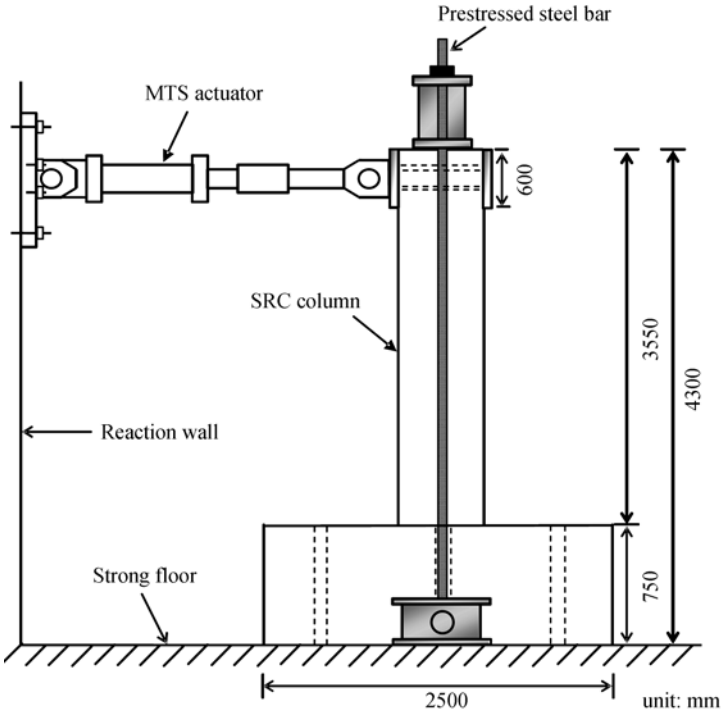

Figure 9 The setup for the SRC column cyclic loading test.

3.3.1 Test devices. (1) Lateral force. An MTS hydraulic actuator was used to impose horizontal lateral force, whose maximum force is 980 kN and maximum stroke is ±200 mm.

(2) Axial force jack. Maximum force output is 980 kN, provides fixed-value axial pressure of the SRC column.

(3) Capital beam. Capital beam is an H-type steel, whose function is smooth transmission of axial force to the specimen.

(4) Hinged bearing of column base. Hinged bearing consists of U-type upper bearing plate, lower bearing plate and circular steel bar connected in series. When axial force and lateral force are applied simultaneously, the axial force screw crossing the two ends of the hinged bearing can be rotated depending on the stress balancing of the upper bearing plate to avoid snap caused by excessive strain of the axial force screw or vanish of axial force caused by screw shortening.

(5) Pre-stressed steel bar. Each of two 39 mm-diameter pre-stressed steel bar groups consists of two 4-m steel bars connected through splicer. Its main function is to splice capital beam and hinged bearing and facilitate transmission of axial compression by the axial force jack to the specimen.

3.3.2 Test method. Single-column cyclic loading tests were conducted. Before the application of cyclic horizontal lateral force, axial pressure was fixed at $0.1(P_n)_{SRC}$ to simulate static load on the SRC column, where $(P_n)_{SRC}$ was the nominal compressive strength of the SRC column, whose value was calculated in accordance with Taiwan SRC Code. The MTS hydraulic actuator fixed on the reaction wall applied cyclic force to the SRC column to simulate the horizontal seismic force on the column. Displacement control was applied to the loading process, loading was repeated for two cycles at each set location, and the loading process is shown in Figure 10 and Table 3. At the final stage of the test, when the lateral bearing force of the SRC column reduced to 80% of the maximum lateral strength, or the drift angle of the specimen reached 6.0% radians, the test ended.

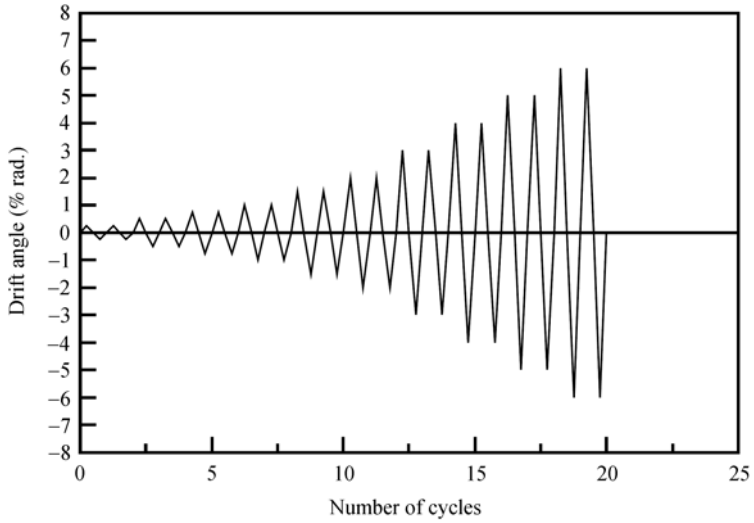

Figure 10 The cyclic loading history.

On the capital beam, two groups of steel bars and hydraulic jacks applied pre-stress to the SRC column, and the connecting part of the steel bars and the hinged bearing might rotate with the horizontal loading displacement process. Although the axial force was applied to the capital, the

Table 3 Cyclic loading history for the SRC column tests

Drift angle(% radian)	Lateral displacement of columns (mm)	Number of cyclic loading
0.25	8.1	2
0.50	16.3	2
0.75	24.4	2
1.00	32.5	2
1.50	48.8	2
2.00	65.0	2
3.00	97.5	2
4.00	130.0	2
5.00	162.5	2
6.00	195.0	2

extension line along the axial force acting direction would not pass the centroid of the column due to the horizontal loading displacement, which resulted in additional bending moment or P–Δ effect, as shown in Figure 11. Therefore, given a lateral displacement δ caused by the horizontal hydraulic actuator, a rotation angle θ is generated from the vertical plane in the axial force acting direction. If the axial force P_a splits into horizontal component $P_a \sin\theta$ and vertical component $P_a \cos\theta$, the secondary moment $M_{P-\Delta}$ caused by the axial force can be calculated as follows:

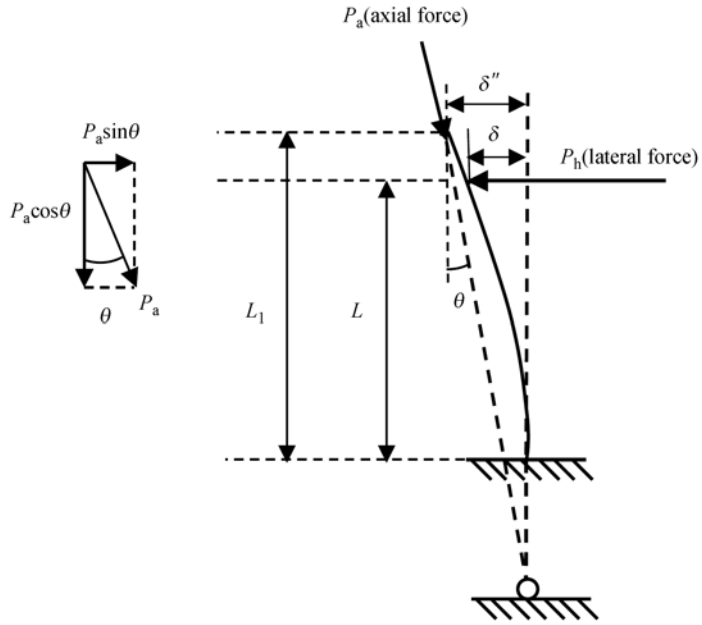

Figure 11 Illustration of the P–Δ effect.

$$M_{P-\Delta} = P_a \cos\theta \times \delta'' - P_a \sin\theta \times L_1, \tag{17}$$

where δ'' is the lateral displacement of the capital, L_1 is the distance between the capital and the column base, and L is the distance between the point of the application of the lateral force and the column base. Relative to the secondary moment $M_{P-\Delta}$, the additional lateral force $P_{P-\Delta}$ caused by the P–Δ effect is

$$P_{P-\Delta} = \frac{M_{P-\Delta}}{L}. \tag{18}$$

Thus the total lateral force $(P_h)_{test}$ acting on the SRC column is calculated as follows:

$$(P_h)_{test} = P_h + P_{P-\Delta} \tag{19}$$

where P_h is the lateral force applied by the hydraulic actuator. Therefore, the total bending moment acting on the SRC column is the total lateral force $(P_h)_{test}$ multiplied by the distance between the lateral force application point and the center of the plastic hinge of SRC column near the column base.

4 Test results and discussions

4.1 Test observations

4.1.1 Specimen C-SRC1. In the early stage of the test, when the drift angle θ of the SRC column reached 0.5% radians, fine horizontal cracks were observed near the column base. When θ reached 1.0% radians, the original cracks continued to extend. When θ reached 2.0% radians, vertical cracks started to be generated. When θ reached the first cycle of 3.0% radians, vertical cracks continued to extend and concrete cracks became more visible; when θ reached the second cycle, concrete cover at the column base started to slightly flake off.

Towards the end of the test, when θ reached 4.0% radians, crack depth on the tension side of the column body increased by about 5 mm. When θ reached the first cycle of 5.0% radians, concrete in the plastic hinge zone at the column base further flaked off. When the drift angle of the SRC column reached 6.0% radians, the test ended. At that time, concrete cover near the column base tangibly flaked off, but the concrete confined by the 5-spirals in SRC column remained intact, the longitudinal reinforcements did not buckle, nor did the spirals break. Figures 12(a) and (b) show the specimen conditions when the drift angle reached 3.0% and 6.0% radians.

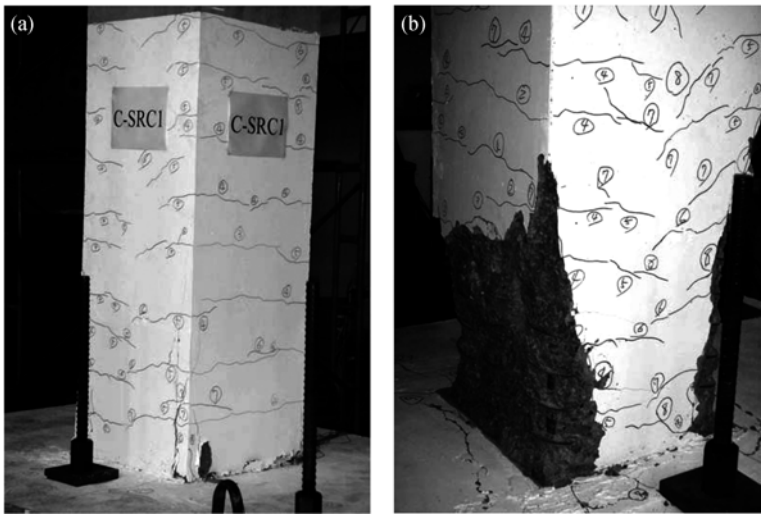

Figure 12 Specimen C-SRC1 when drift angle reached 3.0% and 6.0% radians. (a) Drift angle reached 3.0% radians; (b) drift angle reached 6.0% radians.

4.1.2 Specimen C-SRC2. When the drift angle θ of the SRC column reached 0.5% radians, fine horizontal cracks appeared near the column base. When θ reached 1.0% radians, the original

cracks continued to extend. When θ reached 1.5% radians, the original cracks continued to extend and cracks of concrete became visible on the interface of the column base and foundation. When θ reached 2.0% radians, vertical cracks appeared and slight cracks of concrete became visible on the column base. When θ reached 3.0% radians, concrete cracks on the column base increased, vertical cracks continued to extend; when it reached the second cycle, concrete cover on the column base started to flake off.

When θ reached the first cycle of 4.0% radians, crack depth on the tension side of the column body increased. When θ reached the second cycle, concrete further flaked off. When θ reached 5.0% radians, concrete cover in the plastic hinge zone at the column base tangibly flaked off sheet by sheet.

The test ended when the drift angle of the SRC column reached 6.0% radians. Figures 13(a) and (b) show the specimen conditions when the drift angle reached 3.0% and 6.0% radians. When the test ended, concrete cover near the column base tangibly flaked off, but the concrete confined by the 5-spirals in SRC column remained intact, the longitudinal reinforcement did not buckle, nor did the spirals break, as shown in Figure 14(a) and (b).

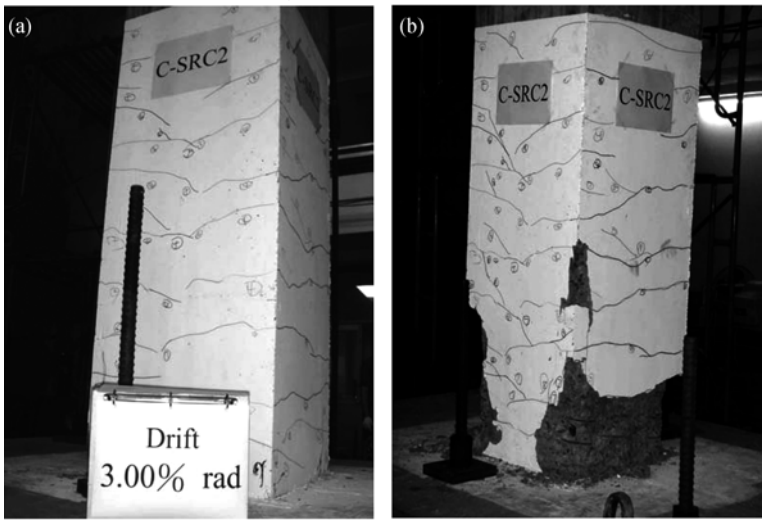

Figure 13 Specimen C-SRC2 when drift angle reached 3.0% and 6.0% radians. (a) Drift angle reached 3.0% radians; (b) drift angle reached 6.0% radians.

4.1.3 Specimen C-SRC3. In the early stage of the test, when the drift angle θ of the SRC column reached 0.75% radians, fine horizontal cracks appeared near the column base. When θ reached 1.0% radians, horizontal cracks continued to extend. When θ reached 2.0% radians, vertical cracks appeared and cracks of concrete became visible on the interface of the column base and foundation, and slight cracks appeared on the column base. When θ reached 3.0% radians, vertical cracks continued to extend, concrete cover on the column base slightly cracked.

Towards the end of the test, when θ reached 4.0% radians, concrete in the pressure area slightly flaked off, crack depth on the tension side of the column body increased by about 8 mm. When θ reached 5.0% radians, concrete cover in the plastic hinge zone at the column base flaked off sheet by sheet. When the drift angle of the SRC column reached 6.0% radians, the test ended. Concrete cover near the column base tangibly flaked off at the time, but the concrete confined by the

5-spirals in SRC column remained intact, the longitudinal reinforcement did not buckle, nor did the spirals break. Figures 15(a) and (b) show the specimen conditions when the drift angle reached 3.0% and 6.0% radians.

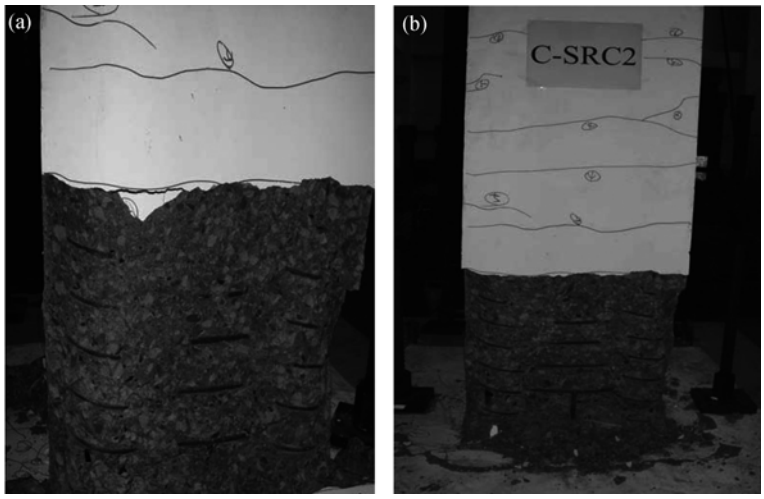

Figure 14 Concrete confined by 5-spirals at plastic deformed zone of specimen C-SRC2. (a) Concrete cover flake-off at plastic zone; (b) main reinforcements and spirals maintained in good conditions.

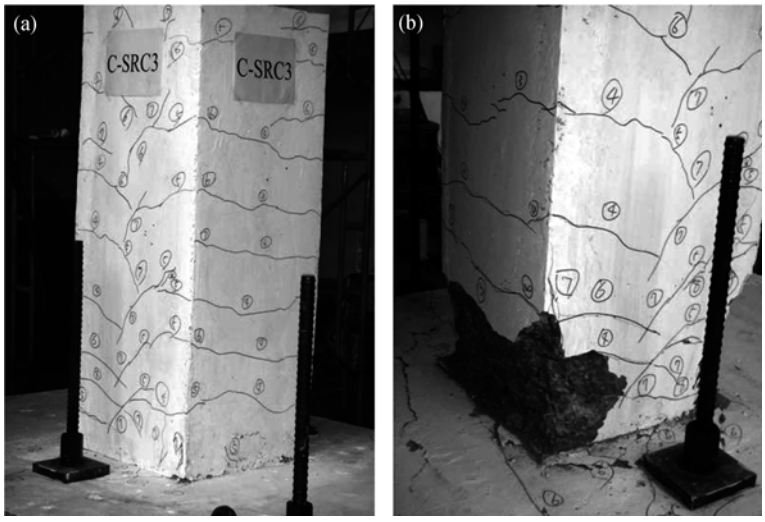

Figure 15 Specimen C-SRC3 when drift angle reached 3.0% and 6.0% radians. (a) Drift angle reached 3.0% radians; (b) drift angle reached 6.0% radians.

4.1.4 Specimen C-SRC4. When the drift angle θ of the SRC column reached 0.75% radians, fine horizontal cracks appeared near the column base. When θ reached 1.0% radians, fine horizontal cracks continued to extend. When θ reached 2.0% radians, vertical cracks appeared and cracks of concrete became visible on the interface of the column base and foundation, and slight cracks appeared on the column base. When θ reached 3.0% radians, vertical cracks continued to extend, concrete cover on the column base slightly cracked.

When θ reached 4.0% radians, concrete on the column base continued to flake off, when it reached the second cycle, vertical cracks became visible in the longitudinal reinforcement direction, and some of concrete cover flaked off. When θ reached 5.0% radians, concrete cover in the plastic hinge zone at the column base flaked off sheet by sheet.

The test ended when the drift angle of the SRC column reached 6.0% radians. Concrete cover near the column base tangibly flaked off at the time, but the concrete confined by the 5-spirals in SRC column remained intact, the longitudinal reinforcement did not buckle, nor did the spirals break. Figures 16(a) and (b) show the specimen conditions when the drift angle reached 3.0% and 6.0% radians.

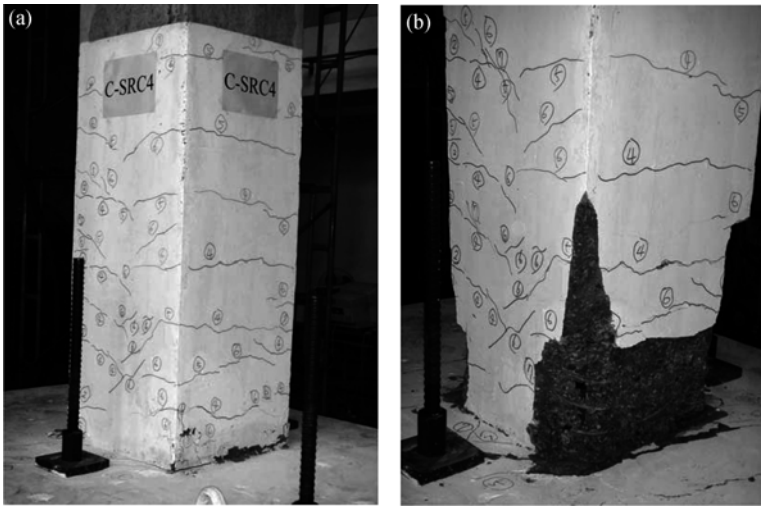

Figure 16 Specimen C-SRC4 when drift angle reached 3.0% and 6.0% radians. (a) Drift angle reached 3.0% radians; (b) drift angle reached 6.0% radians.

However, what is worth noting is that the foregoing observations were carried out according to the test results of SRC columns in this research. The axial force applied to SRC columns in the test was $0.1(P_n)_{SRC}$, the axial force on the columns in a real structure may be larger. Under the action of large axial force, SRC columns in destruction may not be as satisfactory as what is previously described "no buckling of longitudinal reinforcement, no break of spiral and no tangible flake-off of concrete cover."

4.2 Hysteresis loops of SRC columns

Figures 17 to 20 show the hysteresis loops of the four SRC columns under cyclic horizontal loading. The variations of the "lateral force versus displacement" and the "bending moment versus drift angle" can be clearly observed from these figures. It is seen that the hysteresis loops of the four SRC columns are very saturated, indicating the SRC columns have excellent capability of seismic resistance.

It is especially noteworthy that the test results suggested that with the drift angle up to 6.0% radians, the 5-spiral SRC columns having very steady strength were able to effectively resist horizontal shear caused by seismic force without rapid collapse, a feature of paramount importance to safety on the outbreak of a major earthquake.

Figures 17 to 20 show hysteresis loops of SRC columns displaying mutual symmetry of the

first quadrant and the third quadrant, indicating that the specimen underwent similar mechanical behaviors of positive bending moment and negative moment under cyclic loading. Besides, when the drift angle θ of the specimen reached 3% radians, slight pinching appeared on the hysteresis loop because of gradual crack of concrete on the column base; nevertheless, the SRC column strength did not decline due to pinching. From these figures, we can obtain the maximum horizontal lateral force the SRC column resists when the drift angle θ reached 6.0%, with values running as follows: the specimen C-SRC1 is 623 kN, the specimen C-SRC2 is 652 kN, the specimen C-SRC3 is 649 kN, and the specimen C-SRC4 is 628 kN.

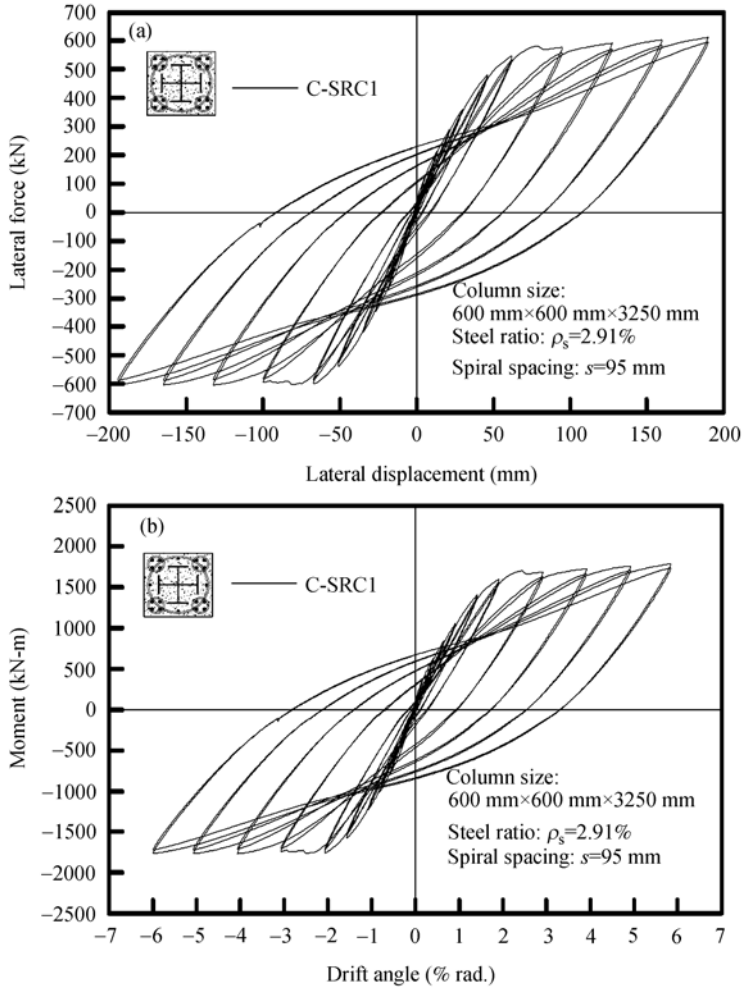

Figure 17 Hysteresis loops of the specimen C-SRC1 subjected to cyclic loading. (a) Force-displacement relationship; (b) moment-rotation relationship.

Figures 21 to 24 are hysteresis loop envelops of the four SRC columns under cyclic loading. These figures show that the SRC column roughly remains elastic before the drift angle θ reaches 1.0% to 1.5% radians, and then gradually enters the inelastic stage. When θ reaches 2.0% radians, inelastic deformation appears on the SRC column base, which slows down strength rise to gradual approach to the plastic stage, approaching to a horizontal line. The figures show that in the plastic stage, the SRC column strength can still sustain and stabilize at a high level without the trend of tangible decline, indicating that the SRC column confined with the 5-spirals has

trend of tangible decline, indicating that the SRC column confined with the 5-spirals has superior strength, toughness and seismic resistance.

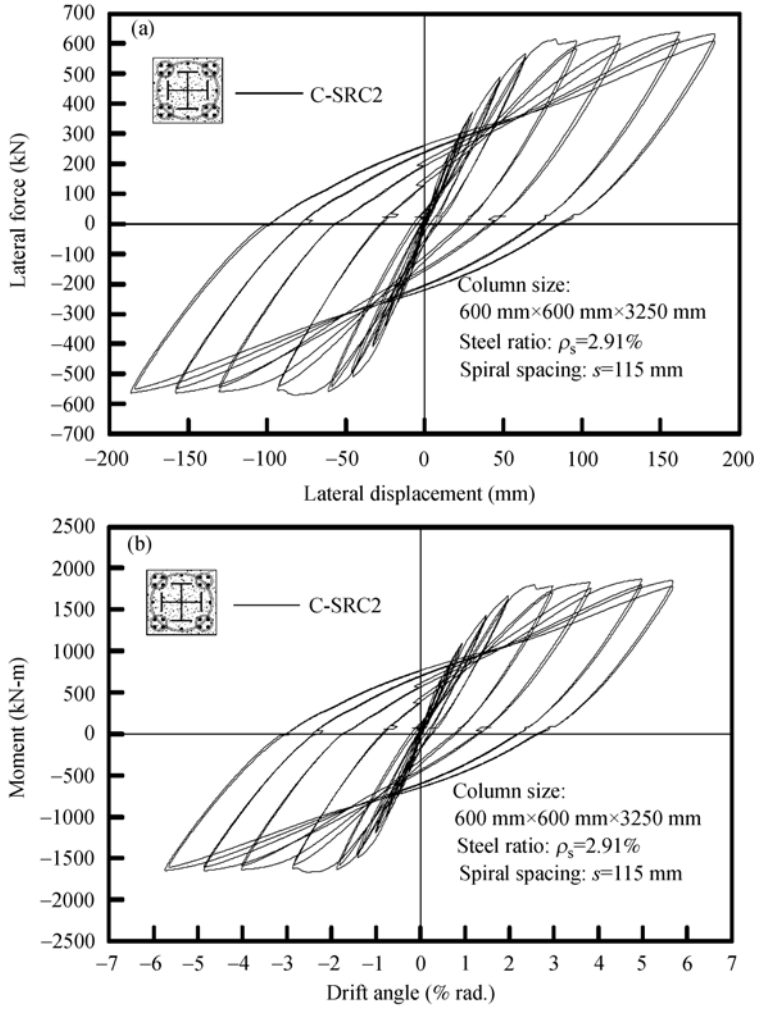

Figure 18 Hysteresis loops of the specimen C-SRC2 subjected to cyclic loading. (a) Force-displacement relationship; (b) moment-rotation relationship.

Furthermore, Figures 25 and 26 show changes in readings of the strain gauges for steel flanges, main reinforcements and spirals of the specimens C-SRC1 and C-SRC2 at the column base (300 mm from the foundation) in cyclic loading. These figures suggested that when the drift angle reached 1.2% radians, the main reinforcement on the outmost reached yield and the steel started to yield from the outer edge of the flange when θ reached 2.0% radians (the yield strain of the main reinforcement was about 2200×10^{-6}). It roughly met what was observed on the hysteresis loop envelopes of Figures 21 to 24, indicating that the SRC column roughly maintained the elastic stage when the drift angle reached 1.0% to 1.5% radians and inelastic deformation (steel flanges started to yield) was tangible when θ reached about 2.0% radians.

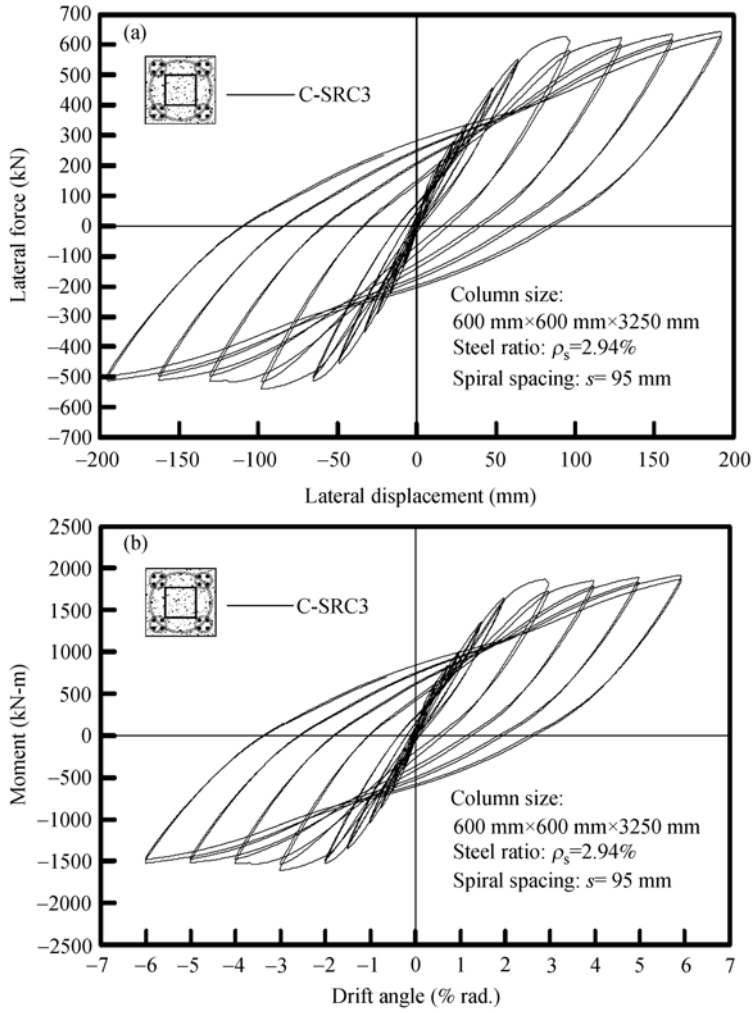

Figure 19 Hysteresis loops of the specimen C-SRC3 subjected to cyclic loading. (a) Force-displacement relationship; (b) moment-rotation relationship.

4.3 Comparisons of design formulas of confining spirals

In confining spiral reduction for SRC columns in the Taiwan SRC Code[21], steel shares part of the SRC column axial force, leading to relative decline of the axial force that concrete has to bear, hence a reduction in SRC column spirals. However, the Code does not consider the role of steel flanges in confining the core concrete in SRC column.

Weng's Formula design method[22] further considers that the "highly confined concrete" in the SRC column may be confined by the steel flanges, while the concrete to be confined with spirals in the SRC column is largely the "ordinary confining concrete", hence relaxed confining spirals in the SRC column. What is characteristic about Weng's Formula is the simultaneous consideration of the "steel consumption" and the "confinement of steel flanges to the core concrete" in the SRC column, and the adoption of a new reduction factor (as shown in Section 3.2) to relax the confining spirals required for the SRC column.

As shown in Table 1, the two foregoing methods were employed in designing confining spirals of the SRC column speciments, with results as follows:

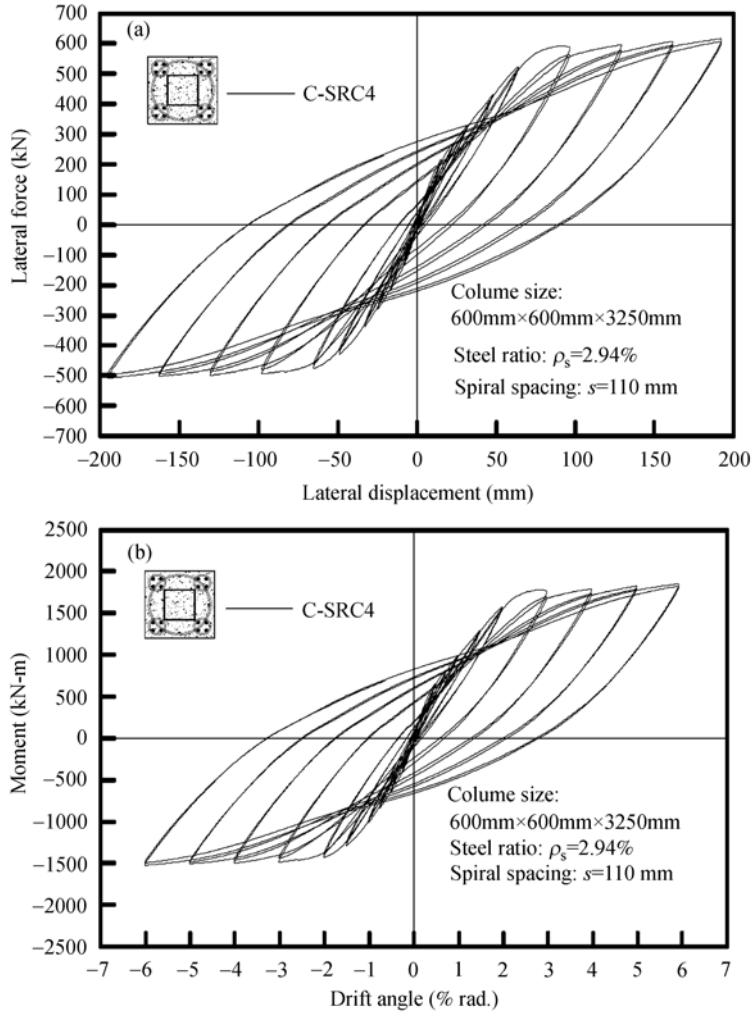

Figure 20 Hysteresis loops of the specimen C-SRC4 subjected to cyclic loading. (a) Force-displacement relationship; (b) moment-rotation relationship.

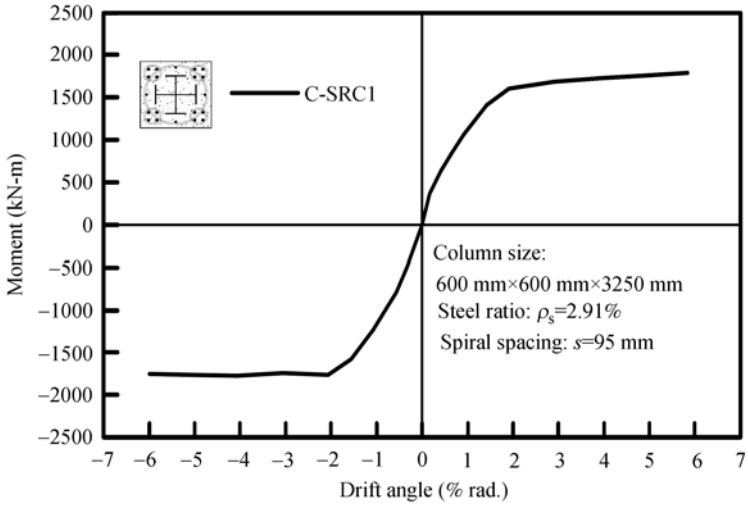

Figure 21 Envelop of the hysteresis loops of the specimen C-SRC1.

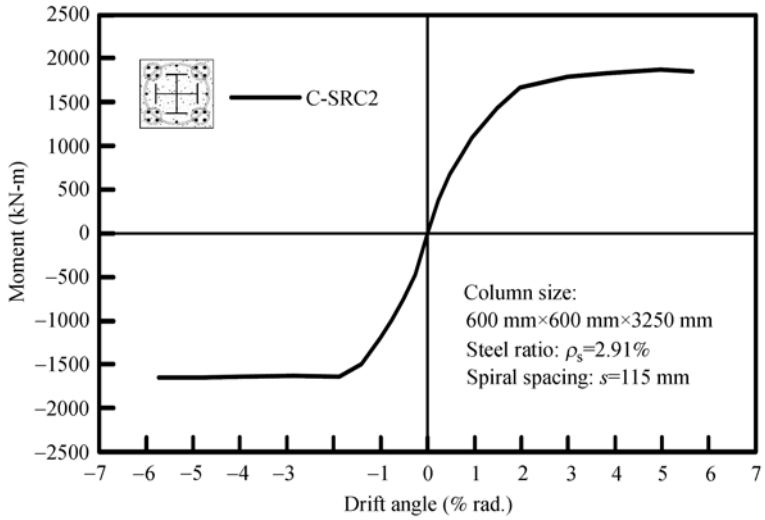

Figure 22 Envelop of the hysteresis loops of the specimen C-SRC2.

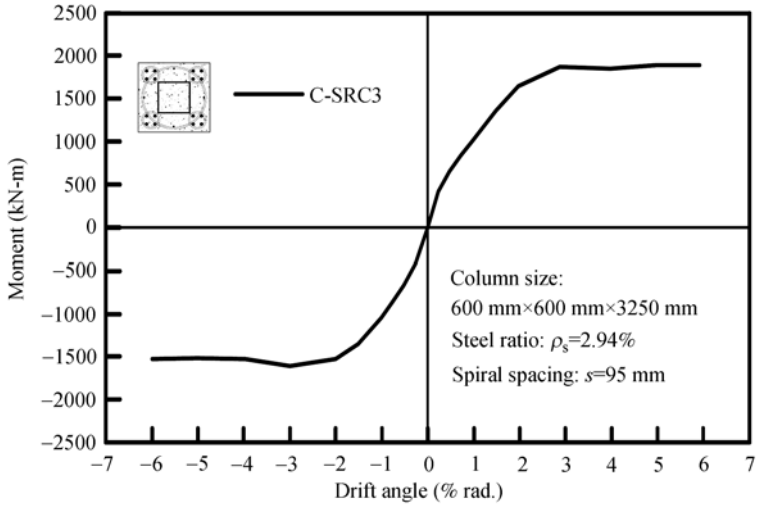

Figure 23 Envelop of the hysteresis loops of the specimen C-SRC3.

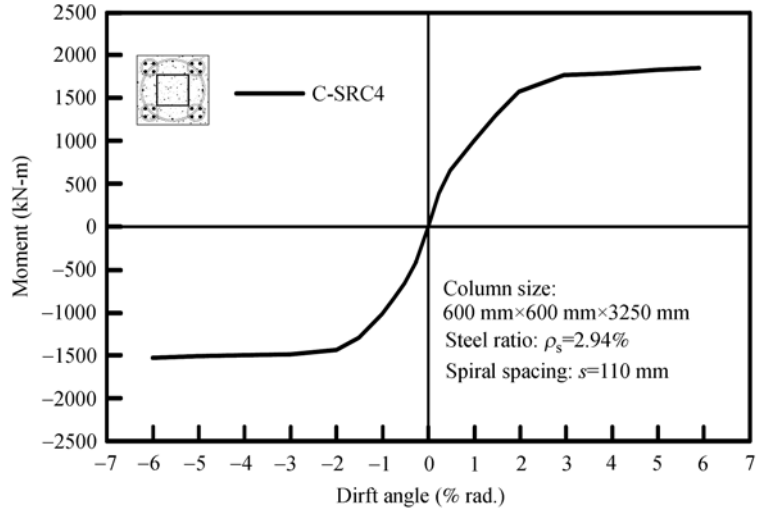

Figure 24 Envelop of the hysteresis loops of the specimen C-SRC4.

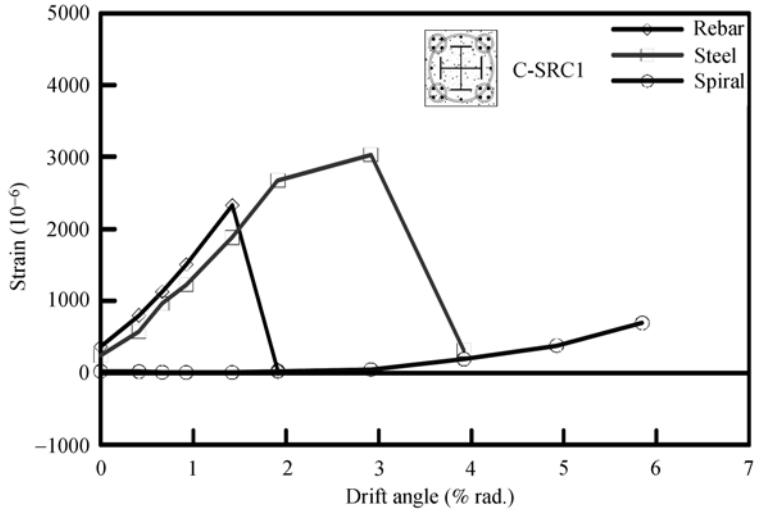

Figure 25 Variations of the strains recorded from specimen C-SRC1. (Note: Strain readings were recorded from strain gauges on longitudinal rebar, steel flange and large spiral, located 300 mm from the SRC column base).

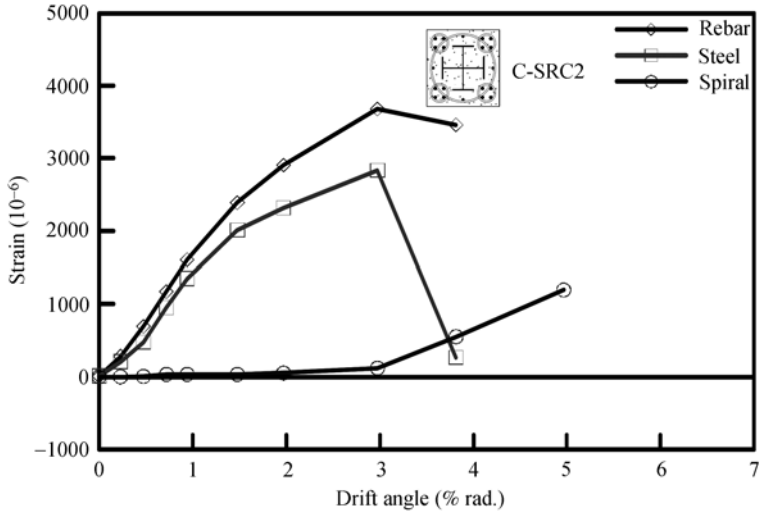

Figure 26 Variations of the strains recorded from specimen C-SRC2. (Note: Strain readings were recorded from strain gauges on longitudinal rebar, steel flange and large spiral, located 300 mm from the SRC column base).

(1) Taiwan SRC Code was applied to design the specimens C-SRC1 and C-SRC3. The spiral spacing was 95 mm; the spiral consumption per unit length was 283 N/m; and the spiral reduction factor was 0.79. The spiral reduction factor represents the ratio of the usage of confining steel calculated in accordance with the Taiwan SRC Code to that of the ACI-318 Code. The smaller the reduction factor, the more saving of the spirals.

(2) Weng's Formula was adopted in designing specimens C-SRC2 and C-SRC4, with fewer spirals required for the two specimens and the spiral spacing was 115 and 110 mm. The spiral consumption per unit length was 235 and 245 N/m, and the spiral reduction factor was 0.65 and 0.68, respectively. The spiral reduction factor represents the ratio of the usage of confining steel calculated in accordance with Weng's Formula to that of the ACI-318 Code.

The test results suggested that although fewer spirals were used in specimens C-SRC2 and

C-SRC4 where Weng's Formula was applied, observations of the hysteresis loops of the four SRC columns in Figures 17 to 20 and the envelops of Figures 21 to 24 indicate that the specimens to which Weng's Formula was applied are satisfactory in strength, toughness and seismic resistance, as good as the SRC column specimens (C-SRC1 and C-SRC3) to which Taiwan SRC Code was applied.

Table 4 makes analysis and comparison of the flexural strengths of the four SRC columns. The comparison shows that the test flexural strengths, $(M_n)_{test}$, of specimens C-SRC2 and C-SRC4 (to which Weng's Formula was applied and fewer spirals were used) are not necessarily weaker than the strengths of specimens C-SRC1 and C-SRC3 (to which Taiwan SRC Code was applied and more spirals were used); where the flexural strength of the specimen C-SRC1 is 1791 kN-m, slightly smaller than 1875 kN-m of the specimen C-SRC2; and the flexural strength of the specimen C-SRC3 is 1915 kN-m, slightly larger than 1853 kN-m of the specimen C-SRC4. In addition, the table also shows the ratios of test flexural strength over nominal flexural strength of the four SRC columns, $(M_n)_{test}/(M_n)_{SRC}$, which comes to 1.27, 1.33, 1.29 and 1.25, respectively, where the values of $(M_n)_{SRC}$ were calculated using the measured material strengths given in Table 2. The ratios indicate that the strengths of the SRC columns confined with 5-spirals are excellent, with over-strength factors ranging from 125% to 133%.

Table 4 Flexural Strength of the SRC columns tested in this study

SRC column cross-section	Specimen designation	P_a(kN) (1)	$P_{P-\Delta}$ (kN) (2)	P_h(kN) (3)	$(P_h)_{test}$(kN) (4)	$(M_n)_{SRC}$(kN-m) (5)	$(M_n)_{test}$(kN-m) (6)	$\frac{(M_n)_{test}}{(M_n)_{SRC}}$
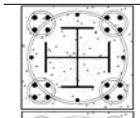	C-SRC1-TWN-95	1380	26	597	623	1414	1791	1.27
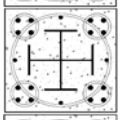	C-SRC2-WENG-115	1380	26	626	652	1414	1875	1.33
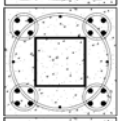	C-SRC3-TWN-95	1380	26	623	649	1483	1915	1.29
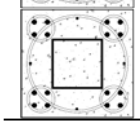	C-SRC4-WENG-110	1380	26	602	628	1483	1853	1.25

Note: (1) P_a is the constant axial load applied to the column, $P_a = 0.1\ P_n$, where P_n is the nominal axial strength of the column calculated according to Taiwan SRC Code. (2) $P_{P-\Delta}$ is the lateral load caused by the P–Δ effect, as given in eq.(18). (3) P_h is he recorded maximum lateral load applied to the column from the MTS actuator. (4) $(P_h)_{test}$ is the total lateral load applied to the column including the P–Δ effect; (4) = (2) + (3). (5) $(M_n)_{SRC}$ is the bending moment which can be resisted by the column while subjected to the axial load P_a, calculated according to Taiwan SRC Code. (6) $(M_n)_{test}$ is the total bending moment applied to the column including the P–Δ effect. The value of $(M_n)_{test}$ is equal to the product of $(P_h)_{test}$ and the distance between the loading point of the lateral force and the center of the plastic hinge of SRC column near the column base.

The test results showed that although Weng's Formula relaxes confining spiral spacing of the SRC column, the strength and ductility of the SRC columns designed with Weng's Formula are as good as the specimens to which Taiwan SRC Code design is applied. The application of rectangular SRC columns confined with 5-spirals plus spiral spacing designed with Weng's Formula may bring about satisfactory seismic resistance and economic benefits for the SRC column. Weng's Formula design method will further rationalize the confining spiral arrangement of the

SRC column, may generate better design results and simplify the construction process of the SRC column hoops. In general, the test results have suggested that with significant saving of the confinement steel, the newly innovated 5-spirals can be successfully applied to the rectangular SRC columns.

Finally, observations of the final conditions of the four SRC columns after the test ended, as shown in Figures 12 to 16, suggested that when the drift angle reached 6% radians, although concrete cover in the plastic zone of the SRC column tangibly flakes off, concrete within the confinement of the 5-spirals remained sound, the longitudinal reinforcements did not buckle, nor did the spirals break. More significantly, the strengths of the four SRC columns were found to be able to sustain and stay at high level without tangible decline trend throughout the entire cyclic loading process. These observations indicated that the 5-spirals provided excellent concrete confinement and prevented the buckling of longitudinal reinforcements.

5 Conclusions

Seismic cyclic loading tests of four full-scale rectangular SRC columns confined with the newly innovated 5-spirals were carried out successfully. The test results showed that the SRC columns enjoy excellent strength, toughness and seismic resistance. As the 5-spirals can be manufactured with automation, they have significant economic benefits and are very suitable for precast construction. Based on the test results, the following conclusions can be drawn within the scope of this study:

(1) For the four SRC columns which underwent seismic cyclic loading tests, their hysteresis loops were very rich, the drift angles of the four SRC columns reached 6.0% radians, indicating rectangular SRC columns confined with 5-spirals have excellent capability in energy dissipation and seismic resistance.

(2) Observations from the tests indicated that the strengths of the four SRC columns were able to sustain and stay high without tangible decline trend throughout the entire cyclic loading process. This phenomenon suggests that the SRC columns confined with 5-spirals are capable of effectively resisting horizontal shear caused by strong earthquake without rapid collapse. This feature is of obvious significance to the safeguarding of lives and properties at the outbreak of major earthquakes.

(3) When the tests ended, observations of the final conditions of the SRC columns found tangible flake-off of concrete cover in the plastic zone near the SRC column base, but concrete within the confinement of the 5-spirals remained sound, the longitudinal reinforcements had no buckling, nor did the spirals break. These observations indicate that the 5-spirals can provide excellent concrete confinement and help to prevent the buckling of longitudinal reinforcements.

(4) With significant saving of the confinement steel, the test results showed that although the Weng's Formula relaxes the confining spiral spacing, the strength and ductility of the SRC columns designed with the Weng's Formula are as good as those specimens designed in accordance with the Taiwan SRC Code. Thus the application of rectangular SRC columns confined with the 5-spirals plus the spiral spacing designed with the Weng's Formula may generate satisfactory seismic resistance and economic benefits for the SRC columns.

1 Weng C C. Characteristics of Taiwan's first design code for steel reinforced concrete building structures. Civil & Hydraul Eng (Taiwan) (in Chinese), 2005, 32(5): 54－62

2 Chang K C, Yin Y L, Wang J C, et al. Experimental study of spiral application to rectangular columns. Engineering (Taiwan) (in Chinese), 2005, 78(3): 101－124
3 Wang B S. Studies on confinement of new rectangular concrete column. Master Dissertation, Institute of Civil Engineering, Taiwan University (in Chinese), 2004
4 Weng C C, Yen S Y, Lin J C. Influence of steel section on confinement reinforcements of SRC columns. J Civil & Hydraul Eng (Taiwan) (in Chinese), 1998, 10(2): 193－204
5 Nakamura T, Wakabayashi M. A study on the superposition method to estimate the ultimate strength of steel reinforced concrete column subjected to axial thrust and bending moment simultaneously. Bulletin of the Disaster Prevention Research Institute, Kyoto University, 1976, 26(242): 163－193
6 Furlong R W. AISC columns design logic Makes sense for composite Column, too. AISC Eng J, 1976, First Quarter: 1－7
7 Furlong R W. Column rules of ACI, SSLC and LRFD compared. ASCE J Struct Eng, 1983, 109(10): 2375－2386
8 Hamdan M, Hunaiti Y. Factors affecting bond strength in composite columns. Proc of the 3rd Inter Conference on Steel-Concrete Composite Structures, Fukuoka, Japan, 1991, 213－218
9 Wakabayashi M. Research on earthquake resistant capacity of composite structures using high strength steel. Proc. of the 10th World Conference on Earthquake Engineering, Balkema, Rotterdam, 1992, 3425－3430
10 Mirza S A, Skrabek B W. Reliability of short composite beam-column strength interaction. ASCE J Struct Eng, 1991, 117(8): 2320－2339
11 Mirza S A, Skrabek B W. Statistical analysis of slender composite beam-column strength. ASCE J Struct Eng, 1992, 118(5): 1312－1332
12 Ricles J M, Paboojian S D. Seismic performance of steel encased composite columns. ASCE J Struct Eng, 1994, 120(8): 2474－2494
13 Mirza S A, Hyttinen V, Hyttinen E. Physical tests and analyses of composite steel-concrete beam-columns. ASCE J Struct Eng, 1996, 122(11): 1317－1326
14 Mirza S A, Tikka T K. Flexural stiffness of composite columns subjected to major axis bending. ACI Struct J, 1999, 96(1): 19－28
15 Mirza S A, Lacroix E A. Comparative strength analyses of concrete-encased steel Composite *c*olumns. ASCE J Struct Eng, 2004, 130(12): 1941－1953
16 Tikka T K, Mirza S A. Equivalent uniform moment diagram factor for composite columns in major axis bending. ASCE J Struct Eng, 2005, 131(4): 569－581
17 Tikka T K, Mirza S A. Nonlinear equation for flexural stiffness of slender composite columns in major axis bending. ASCE J Struct Eng, 2006, 132(6): 387－399
18 Yin Y L, Weng C C, Wang J C, et al. Experimental study on application of 5-spirals to rectangular SRC columns. Struct Eng (Taiwan) (in Chinese), 2007, 22(3): 3－27
19 American Concrete Institute. Building Code Requirements for Structural Concrete and Commentary (ACI 318M-05), Farmington Hills, Michigan, 2005
20 American Institute of Steel Construction. Seismic Provisions for Structural Steel Buildings, Chicago, Illinois, 2005
21 Taiwan Construction and Planning Agency. Design Code and Commentary for Steel Reinforced Concrete Structures (in Chinese). Taibei, 2004
22 Weng C C, Wang H S, Li R, et al. Experimental study and seismic resistance design of confining hoops for steel reinforced concrete columns. Struct Eng (Taiwan) (in Chinese), 2006, 21(3): 55－83
23 Weng C C. The development of design code for steel reinforced concrete building structures in Taiwan. Struct Eng (Taiwan) (in Chinese), 2005, 20(1): 3－30